INFLUENCE OF SPATIAL ATTENTION ON THE RECEPTIVE FIELD SHAPE OF NEURONS IN MONKEY AREA MT

Jérémy Fix
IMS, SUPELEC
F-57070 Metz, France
email: jeremy.fix@supelec.fr

Henning Schroll
Department of Psychology, Westf. Wilhelms-University
D-48149 Munster, Germany
email: henning.schroll@uni-muenster.de

Katharina Anton-Erxleben
Department of Psychology
Center for Neural Science, New York University
New York, NY 10003, United States of America
email: katharina.antonerxleben@nyu.edu

Thilo Womelsdorf
Laboratory for Neural Circuits and Cognitive Control
Centre for Brain and Mind, Robarts Research Institute
London, Ontario, Canada
email: thiwom@imaging.robarts.ca

Stefan Treue
German Primate Center
37073 Gottingen, Germany
email: treue@gwdg.de

Fred H. Hamker
Artificial Intelligence, Chemnitz University of Technology
09107, Chemnitz, Germany
email : fred.hamker@informatik.tu-chemnitz.de

ABSTRACT
Spatial attention has been shown to produce non-multiplicative effects on visual receptive fields(vRFs) in monkey area MT, including shift and shrinkage [1]. These non-multiplicative effects have been recently explained by a multiplicative model of attention [2]. However, Womelsdorf et al. introduced a simplification leading to two distinct models, one for unmodulated and another for modulated responses. We provide here a unified account of both the unmodulated and modulated responses within a single model. This model relies on a divisive influence of anti-preferred stimuli placed within the receptive fields of the neurons scaled by spatial attention. This model also allows to reproduce the influence of spatial attention observed in [3] and provides physiological explanation for the differential shift for the centre and surround of the receptive field.

KEY WORDS
attention, receptive field, suppression, gain modulation, area MT.

1 Introduction

Visual attention is a property of the brain to focus on relevant visual information while ignoring non-relevant information. While important results about visual attention have been gathered both in psychology and electrophysiology [4, 5], the neuronal mechanisms involved in visual attention remain unclear. At the single cell level, it has been proposed that spatial attention acts as a multiplicative gain on feedforward sensory inputs [6], facilitating the processing of behaviourally relevant spatial locations. While some attention-related effects (scaling of the tuning curve, contrast sensitivity increase) are consistent with a multiplicative influence of attention, other effects such as shift and shrinkage of the receptive fields (RFs), as observed in [1, 3], seem to be incompatible with it at first sight (but see [7] for a qualitative account to model peri-saccadic RF shifts).

Womelsdorf et al. [2] applied a standard computational model to explain the shift and shrinkage of the receptive fields as observed in monkey area MT [1]. This model relies on a multiplicative gain increase $\mathbf{g}(x, y) \cdot gain$ of the Gaussian response profile $\mathbf{g}(x, y)$, where $gain = 1 + g_{Att}(x, y)$ and $g_{Att}(x, y)$ a Gaussian attentional focus. Analysing the experimental data revealed that RF flanks opposite to the focus of attention are suppressed by attention. To obtain the suppression of the flank, the authors introduced a simplification which led to two different models for explaining the unmodulated and modulated responses. We propose here a unified account of the unmodulated and modulated responses by formulating a single model used to reproduce the data in the two conditions. The model explicitly considers the influence of the attended stimulus and not just the response to the probe. The attended stimulus, a random dot pattern moving in the anti-preferred direction of the recorded cell, is proposed to exert a suppressive influence on the response of the cell, magnified by spatial attention. In addition, we show that a small modification of the model allows also to account for the other data [3] where attention was hypothesized to shift differently the centre and the surround of the receptive field.

2 Materials and methods

2.1 Experimental paradigm

The experimental data used in this study were recorded by [1]. Two monkeys performed an attentional task while the

response neurons was recorded in area MT. Here we briefly summarize the experimental paradigm, more detailed information is provided in the original paper [1]. The stimuli used for the experiment are random dot patterns of small bright dots plotted within a stationary circular aperture on a dark monitor. A trial started when the monkey foveated a small square presented on the screen. Then, a cue, a stationary random dot pattern was presented. By its location, the cue indicated the future position of the task relevant stimulus. After a certain delay, three stimuli were presented. Two stimuli were presented within the receptive field of the recorded cell (denoted S1 and S2). A third stimulus was presented in the opposite hemifield. These three stimuli (S1, S2 and S3) were of low contrast and moving in the anti-preferred direction of the recorded cell. Two conditions were considered. In the first condition, the monkey had to detect a small transient change of movement direction of S3. This condition is called *attend-away* condition. In the second condition, the monkey had to detect a small transient change of movement direction of S1 or S2. This second condition is called *attend-in* condition. When required, we call the *attend-in* condition *attend-S1* or *attend-S2* condition. During the attentional task, probes were quickly flashed on a regular grid to map the receptive field of the cell. The probes were moving in the preferred direction of the cell and were of higher contrast than the anti-preferred stimuli. The dataset contains recordings of 97 pairs of attend-away/attend-in conditions.

2.2 Model

We propose a dynamical model from which we derive the steady state equations used in this study. The response r_{unmod} of a cell, to a probe flashed at position (x, y) is modelled as a two-dimensional elliptical Gaussian :

$$r_{unmod}(x,y) = A \cdot \mathbf{g}(x,y) + B \tag{1}$$

$$\begin{aligned}\mathbf{g}(x,y) = \exp(\quad & - \quad \frac{\left[(x-x_0)\cdot\cos(\theta) + (y-y_0)\cdot\sin(\theta)\right]^2}{2\sigma_x^2} \\ & - \quad \frac{\left[-(x-x_0)\cdot\sin(\theta) + (y-y_0)\cdot\cos(\theta)\right]^2}{2\sigma_y^2}\end{aligned}$$

with (x_0, y_0) the RF centre, θ the orientation of its main axis, σ_x and σ_y the standard deviations respectively along the major and minor axis, A the maximal response of the cell and B its baseline (i.e. the response of the cell to a probe flashed far away from its receptive field centre, in the absence of the anti-preferred stimuli S1 and S2). The spatial attention signal is modelled as a two-dimensional circular symmetric Gaussian centred at (x_{Att}, y_{Att}), of amplitude A_{Att} and variance σ_{Att} :

$$g_{Att}(x,y) = A_{Att} \cdot \exp(-\frac{(x-x_{Att})^2 + (y-y_{Att})^2}{2\sigma_{Att}^2}) \tag{2}$$

The evolution of the activity $r(t)$ of the cell is defined with the following first order differential equation :

$$\begin{aligned}\tau\frac{dr}{dt}(t) = \quad & - \quad r(t) + A\cdot\mathbf{g}(x,y).(1+g_{Att}(x,y)) \\ & - \quad r(t).A_{s1}\cdot\mathbf{g}(x_{s1},y_{s1}).(1+g_{Att}(x_{s1},y_{s1})) \\ & - \quad r(t).A_{s2}\cdot\mathbf{g}(x_{s2},y_{s2}).(1+g_{Att}(x_{s2},y_{s2})) \\ & + \quad B\end{aligned} \tag{3}$$

Spatial attention is introduced as a multiplicative factor modulating the feedforward sensory inputs of the cell [8]. The feedforward sensory inputs come from the probe $A \cdot \mathbf{g}(x, y)$ as well as from the anti-preferred stimuli S1 ($A_{s1} \cdot \mathbf{g}(x_{s1}, y_{s1})$) and S2 ($A_{s2}.\mathbf{g}(x_{s2}, y_{s2})$), although S1 and S2 could be of lateral origin. In line with the normalization models of attention [9], the inhibitory influence of the anti-preferred stimuli will appear as a divisive term in the steady state solution if it is modulated by the firing rate of the cell. In the following, we call the *attend-away* condition the condition when attention is directed far away from the receptive field centre and the *attend-in* condition the condition when attention is directed on one of the anti-preferred stimuli within the receptive field of the cell. The experimental dataset consists of pairs of *attend-away* and one *attend-in* responses. Therefore, we neglect in the following the influence of the anti-preferred stimulus that is not directly attended. In addition, since, during the experiment, the position of the anti-preferred stimulus S1 is held fixed, we can simplify equation (3) by introducing $A_1 = A_{s1}\mathbf{g}(x_{s1}, y_{s1})$ which leads to the simplified model:

$$\begin{aligned}\tau\frac{dr}{dt}(t) = -r(t) \quad & + \quad A\cdot\mathbf{g}(x,y)\cdot(1+g_{Att}(x,y)) \\ & - \quad r(t)\cdot A_1\cdot(1+g_{Att}(x_{s1},y_{s1})) \\ & + \quad B\end{aligned} \tag{4}$$

From the previous equation, we can derive the steady state equations for both the *attend-away* and *attend-in* conditions. Since in the *attend-away* condition spatial attention is directed far away from the receptive field of the recorded cell, we can omit the attentional term. In this condition, we obtain the response r_{out} defined by:

$$r_{out}(x,y) = \frac{A\mathbf{g}(x,y) + B}{1 + A_1} \tag{5}$$

The steady-state *attend-in* response, denoted by r_{in}, is given by the following equation :

$$r_{in}(x,y) = \frac{A.\mathbf{g}(x,y)\cdot(1+g_{Att}(x,y)) + B}{1 + A_1\cdot(1+g_{Att}(x_{s1},y_{s1}))} \tag{6}$$

In the rest of the paper, we call the model defined by the previous equations the divisive model. We also call the model in which the influence of the anti-preferred stimuli is not introduced ($A_1 = 0$) the Gaussian model. All the analyses were performed with custom scripts written in MATLAB (The MathWorks, Natrick, MA)[1].

[1]The scripts used for the theoretical tuning curves (figures 1A and 4)

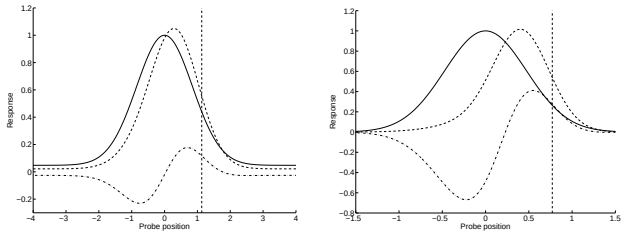

A B

Figure 1: Illustration of the RF changes when attending away (solid line) or attending the anti-preferred stimulus $S1$ (dashed line). The position of $S1$ is indicated by the vertical dashed line. As seen on the difference between the *attend-in* and *attend-away* conditions (dashed-point line), the response to a probe flashed on the same flank as $S1$ is increased while the response to a probe flashed on the opposite flank is decreased. A) Simulation of a 1D model with the parameters $A = 2$, $B = 0.1$, $\sigma_x = 15$, $x_0 = 0$, $x_{Att} = 20$, $A_{Att} = 2$, $\sigma_{Att} = 20$, $x_{s1} = 20$. B) Response of one of the fitted cell (Cell #8 with the statistics $R_2^{out} = 0.87$, $R_2^{in} = 0.79$), along the axis connecting the RF's center to the anti-preferred stimulus $S1$. For both illustrations, the x-axis is scaled by the unmodulated RF size and the y-axis is scaled by the maximal *attend-away* response.

2.3 Illustrative example in one dimension

We here illustrate the RF shape change by a one-dimensional example. The equations used for the simulation are the equations (5) and (6) expressed in one spatial dimension. The receptive fields when attending away (solid line) or attending S1 (dashed line) are shown on figure 1A. As seen from the difference between the *attend-S1* and *attend-away* conditions (dashed-dot line), the response to a probe flashed close to the attended stimulus S1 is increased, while the response to a probe flashed on the opposite flank of the receptive field is decreased. The suppressive effect of attention on the left flank is due to an increase of the inhibitory drive from the anti-preferred stimulus that is not compensated by an increase of the excitatory drive from the probe: when attention is on $S1$ and a flash is presented on the left flank, the inhibitory drive from $S1$ is magnified while the excitatory drive from the probe is less influenced by attention. The net effect is therefore suppressive. When a probe is flashed on the flank of the receptive field closer to attention, the attentional effect on the probe is larger than on S1. To illustrate this effect on a recorded cell, the figure 1B shows a slice of the *attend-away* and *attend-in* responses of one cell fitted with the two-dimensional model. As seen from the difference between the two responses (dashed-point line), when attending $S1$, the response is increased on the flank close to $S1$ and decreased on the opposite flank. The suppression of the flank on the side opposite to $S1$ allows for a strong shift of the RF.

2.4 Fitting procedure

The dataset provided by [1] contains the *attend-away* and one of the two *attend-in* conditions for each cell. We fitted simultaneously the two conditions using the *lsqnonlin* function of MATLAB (The MathWorks), searching for 10 free parameters $(A, B, x_0, y_0, \theta, \sigma_x, \sigma_y, A_{Att}, \sigma_{Att}, A_1)$, repeating the procedure for several times to avoid local minima. For each cell, the minimized criterion is based on the mean square error between the model's response and the experimental data, normalized by their respective standard deviations σ_{out} and σ_{in}. Namely, the following criterion was minimized :

$$\begin{aligned} C = & \sum_i \left(\frac{r_{out}(x_i, y_i) - z_{out}(x_i, y_i)}{\sigma_{out}} \right)^2 \\ + & \sum_i \left(\frac{r_{in}(x_i, y_i) - z_{in}(x_i, y_i)}{\sigma_{in}} \right)^2 \end{aligned}$$

The statistics reported in the result section are the R^2 values for each condition as well as the combined R^2 value for the two conditions :

$$\begin{aligned} R^2_{out} &= 1 - \frac{\sum_i (r_{out}(x_i, y_i) - z_{out}(x_i, y_i))^2}{\sum_i (z_{out}(x_i, y_i) - \bar{z}_{out})^2} \\ R^2_{in} &= 1 - \frac{\sum_i (r_{in}(x_i, y_i) - z_{in}(x_i, y_i))^2}{\sum_i (z_{in}(x_i, y_i) - \bar{z}_{in})^2} \\ R^2_{both} &= \frac{R^2_{out} + R^2_{in}}{2} \end{aligned} \quad (7)$$

2.5 Variability of the feedback signals

As explained above, the fits of a single cell were performed several times with random starting values of the parameters. During the fits, we kept all the parameters that led to a R^2_{tot} of at least 0.99 times the best R^2_{tot}. For some cells, we observed that the shape of the attentional signal of the models we kept may vary significantly. In order to analyse the shape of the feedback signals, we introduce a criterion to exclude the cells for which the shape of the attentional signal exhibits too much variability. We excluded the cells for which the parameters of the feedback signals (amplitude or variance), leading to a model with a R^2_{tot} of at least 0.99 the best R^2_{tot}, had a standard deviation higher than 5% the mean value. This selection criterion led to discard 29 cells out of the 97 recorded cells.

2.6 Analysis

Receptive field size

The RF size is computed as the square root of the area above the half-maximal baseline-corrected response. In

are available on the website of the author : http://jeremy.fix.free.fr/

the *attend-away* condition, the RF size can be computed analytically. Given the RF is elliptic with a major and minor axis of lengths $\sigma_x\sqrt{2\log(2)}$ and $\sigma_y\sqrt{2\log(2)}$, the area above the half-maximum is $2\pi\log(2)\sigma_x\sigma_y$. This leads to an *attend-away* RF size of :

$$s_{RF}^{out} = \sqrt{2\pi\log(2)\sigma_x\sigma_y} \tag{8}$$

The RF size in the *attend-in* condition s_{RF}^{in} was computed by probing on a fine grid the RF. We checked that the response of the cell on the borders of the grid was below the half-maximum response and counted the number of probes falling within the half-maximum area. The square root of the area covered by these probes was used as a measure of the receptive field size. To evaluate the influence of spatial attention on the RF size, we define the variation of receptive field size Δs_{RF} as the ratio between *attend-away* and *attend-in* receptive field sizes:

$$\Delta s_{RF} = 100\frac{s_{RF}^{in}}{s_{RF}^{out}} \tag{9}$$

Therefore, a Δs_{RF} smaller than 100 indicates a shrinkage of the receptive field with attention while a Δs_{RF} higher than 100 indicates an expansion.

Receptive field shift

To evaluate the influence of spatial attention on the position of the RF centre of the cell, we computed the RF shift between the *attend-away* and *attend-in* conditions. The centre of the RF in both conditions was evaluated by searching for the position of the probe that leads to the maximal response of the model cell, using a fine grid of probes (usually with a step of 0.3 degrees). If we denote $\vec{c}_{S1}$ a unitary vector on this axis, $\vec{c}_{out}$ the position of the peak response in the attend-away condition and $\vec{c}_{in}$ the position of the peak response in the attend-in condition, the RF shift Δc is estimated as :

$$\Delta c = \frac{(\vec{c}_{in} - \vec{c}_{out}).\vec{c}_{S1}}{s_{RF}^{out}} \tag{10}$$

A positive Δc indicates a shift of the RF centre toward attention, while a negative shift Δc indicates a shift away from attention.

3 Results

3.1 Quantitative results of the divisive and Gaussian models

The statistics of the different models we tested are shown in table 1. We observed that the performance of the divisive model is significantly better than a Gaussian model (*paired t-test*, $p < 0.001$). The better fits obtained with our model are explained by the introduction of the inhibitory influence of the anti-preferred stimulus which allows to suppress one of the flanks of the receptive field. This suppressive effect

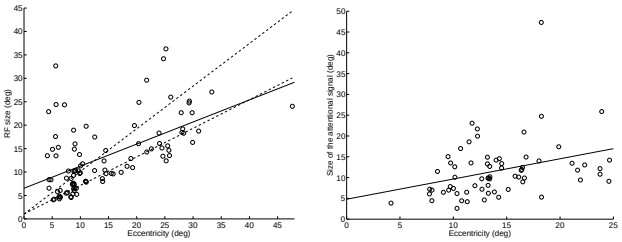

A B

Figure 2: A) Unmodulated receptive field size as a function of the receptive field eccentricity. In addition to a linear fit of the RF size ($6.5^o + 0.47\epsilon$, solid line), the relationships given by [10] ($s_{RF} = 1.04^o + 0.91\epsilon$) and by [11] ($s_{RF} = 1.04^o + 0.61\epsilon$) are plotted, with ϵ the eccentricity of the receptive field centre. B) Size of the attentional signal ($\sigma_{Att}\sqrt{2\pi\log(2)}$) as a function of the attended stimulus' eccentricity. Only the signals for which the variability was small, as explained in section 2.5, are shown. The slope is 0.49 and the y-intercept is 4.8 degrees.

of the anti-preferred stimulus S1 is observed on the flank of the receptive field on the side opposite to $S1$. Although similar effects can be achieved with attentional foci modeled with a DoG, it does not provide a clear understanding of the neural effects.

	R^2_{out}	R^2_{in}	R^2_{both}
Gaussian	0.698 (SD 0.153)	0.745 (SD 0.121)	0.722 (SD 0.127)
Divisive	0.752 (SD 0.099)	0.764 (SD 0.107)	0.757 (SD 0.094)
DoG	0.755 (SD 0.101)	0.778 (SD 0.102)	0.767 (SD 0.093)

Table 1: Statistics of the fitted models with the population mean R^2 values and their respective standard deviations.

3.2 Receptive field size change and shift

We found that the unmodulated receptive field size was increasing approximately linearly with eccentricity according to the relationship $s_{RF}^{out} = 6.5^o + 0.47\epsilon$ (fig. 2). The receptive field size of MT neurons previously reported was $s_{RF} = 1.04^o + 0.91\epsilon$ [10] and $s_{RF} = 1.04^o + 0.61\epsilon$ [11]. The higher y-intercept is due to some receptive fields that are quite large for small eccentricities.

In addition, the figure 3 shows the relationship between the shift and the shrinkage. The more the RF shifts toward attention, the more it shrinks. Expansion of the receptive field is observed only for small shifts. These results are consistent with the shrinkage/shift patterns reported in [2].

3.3 Attentional signal

Our model allows to extract the shape of the attentional signal as a function of the eccentricity of the attended

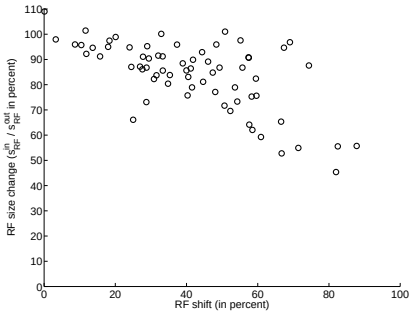

Figure 3: Receptive field shift and shrinkage.

stimulus. The size of the attentional signal computed as the square root of the half-maximum area ($s_{Att} = \sigma_{Att}\sqrt{2\pi \log(2)}$ is shown on figure 2 as a function of the attended target's eccentricity. The size of the attentional signal is growing as a function of eccentricity of the attended stimulus. The slope of the relationship is 0.49 with a y-intercept of 4.8. With a similar slope and y-intercept, the size of the attentional signal is similar to the size of the receptive field.

3.4 The influence of the second anti-preferred stimulus

The recent study of [3] used almost the same experimental paradigm as [1], using a larger grid of probes in order to evaluate the influence of attention on the periphery of the receptive fields of MT neurons. When computing the difference map between the *attend-S1* and *attend-S2* conditions, the authors observed two opposite effects in the centre and periphery of the receptive field. In the centre of the receptive field, the response is increased close to the attended target and decreased further away. The opposite is observed in the periphery. Anton-Erxleben et al. proposed that the observed effects are due to different shifts of the excitatory centre and inhibitory surround of the recorded cells (figure 4). To explain this observation with our model an interaction between the probe and the anti-preferred stimulus is assumed, so that the inhibitory term A_1 in equation (4) is replaced by :

$$A_1 exp(-\frac{(x_{s1}-x)^2+(y_{s1}-y)^2}{2\sigma_{s1}^2}) \qquad (11)$$

This allows to obtain the excitatory and inhibitory components in the periphery. These peripheral effects are here due to a suppression of the baseline response when a probe is flashed close to the attended stimulus (in the difference map, this results in a positive or negative component depending on whether attention is on $S1$ or $S2$). Using this modified model to fit the data of [3] provided good statistics ($R^2_{fix} = 0.796(SD = 0.132)$, $R^2_{in,S1} = 0.815(SD = 0.123)$, $R^2_{in,S2} = 0.805(SD = 0.141)$,$R^2_{tot} = 0.805(SD = 0.123)$). However, the feedback signals revealed to be highly variable. In fact, the dataset does not contain an *attend-away* condition but an *attend-fixation*. For the majority of cells, the fixation stimulus lies within the receptive field of the recorded cell, which forced us to consider all the conditions (*attend-fixation*, *attend-S1* and *attend-S2*) as *attend-in* conditions. This leads to more complicated fits. Unfortunately, the absence of an *attend-away* condition removes constraints on the unmodulated receptive field parameters, which impairs a more detailed analysis as with the other dataset.

An ideal situation would be to have the responses in the *attend-away* condition in the absence of $S1$ and $S2$, *attend-away* condition with $S1$ and $S2$, *attend-S1* and *attend-S2* conditions. We would then be able to fit separately the unmodulated receptive fields before introducing the influences of the anti-preferred stimuli and the influence of spatial attention.

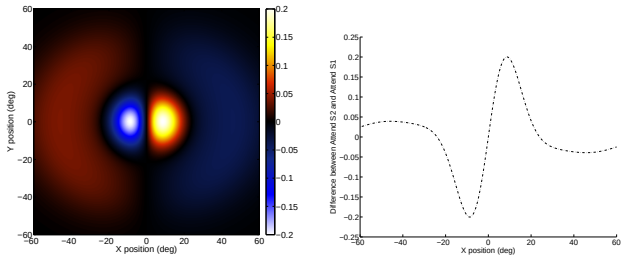

Figure 4: Illustrative example of the difference between the responses when attending S1 ($x_{s1} = 15, y_{s1} = 0$) and the responses when attending S2 ($x_{s2} = -15, y_{s2} = 0$) showing that a divisive model can qualitatively account for the difference maps observed in [3]. In order to produce this pattern, an influence between the probe and the anti-preferred stimuli has been introduced leading to a suppression by the anti-preferred stimuli that is stronger when a probe is flashed close to them. The illustration on the right is a slice of the difference map along the x-axis connecting $S1$, $S2$ and the receptive field centre.

4 Discussion

We have proposed here a unified model accounting for the data of [1]. The model we proposed explains shift and shrinkage of receptive fields by an increase of the response close to attention and a suppression on the opposite flank. The novelty we introduced is the inhibitory influence, through a divisive term, of the anti-preferred stimuli, magnified by spatial attention. We also provide a more physiological explanation of the effects observed in [3]. Anton-Erxleben et al. found a RF change similar to the one illustrated on figure 4. They proposed that this pattern is due to a different shift of the centre and surround of the receptive field. Here we propose that this pattern of change

can be obtained by introducing a divisive inhibitory influence of the anti-preferred stimuli.

Divisive models were previously proposed to model the influence of attention on visual receptive fields [9] or the influence of contrast on the center/surround structure of V1 receptive fields [12, 13]. Another class of models is substractive models. For example, [13] obtained similar results using a substractive or divisive model. Here, we also analyzed a substractive inhibitory model where the attentional signal is a difference of Gaussians (DoG), multiplicatively scaling the sensory feedforward input (i.e. replacing the attentional Gaussian g_{Att} in equation (3) by a difference of Gaussians and removing the influence of the anti-preferred stimulus). This also introduces suppression of the periphery of the receptive field on the opposite side of attention. Indeed, we performed the fits with a DoG model which led to good fitting statistics (see table 1). However, the model's parameters were too variable to report their values. In particular, we observed that the inhibitory component of the DoG attentional signal could be local or broad, up to constant for some cells (i.e. not null for large eccentricities). Indeed, since the receptive field and the attentional signal are interacting multiplicatively in the model, the receptive field is hiding part of the attentional signal. If simultaneous recordings were available for the same attentional conditions, we may have been able to analyse if a DoG model would account for the data. In addition, the divisive and DoG model provide different interpretations for the observed suppression. If the inhibition were purely spatial-based (as in the DoG model), originating from the attentional feedback, it should not depend on the selectivity in feature space of the recorded cell. Therefore, we expect that in this situation, varying the motion direction of the attended anti-preferred stimulus would not change the suppression of the flank. On the opposite, with the divisive model we proposed, the amplitude of the inhibitory influence A_1 is dependent on the selectivity in feature space of the recorded cell and on the motion direction of the anti-preferred stimulus.

Biased competition suggests that attention directed toward a stimulus inside the receptive field of a neuron occupied by two stimuli drives the response of the neuron toward the response to the attended stimulus presented alone. Interestingly, the model studied in this paper suggests different influences of attention depending on the probe position (see for example figure 1B, the probe moving in the preferred direction of the recorded neuron). In particular, attending to $S1$ causes a decrease of the response to a probe flashed on the suppressed flank. On the side close to attention, we observe the opposite effect; the response to a probe flashed close to attention is increased even if an anti-preferred stimulus is attended.

References

[1] T. Womelsdorf, K. Anton-Erxleben, F. Pieper, and S. Treue. Dynamic shifts of visual receptive fields in cortical area mt by spatial attention. *Nat Neurosci*, 9(9):1156–60, 2006.

[2] T. Womelsdorf, K. Anton-Erxleben, and S. Treue. Receptive field shift and shrinkage in macaque middle temporal area through attentional gain modulation. *J Neurosci*, 28(36):8934–44, 2008.

[3] K. Anton-Erxleben, V. Stephan, and S. Treue. Attention reshapes center-surround receptive field structure in macaque cortical area mt. *Cereb Cortex*, 19(10):2466–78, 2009.

[4] J.H. Reynolds and L. Chelazzi. Attentional modulation of visual processing. *Annu Rev Neurosci*, 27:611–47, 2004.

[5] R. Desimone and J. Duncan. Neural mechanisms of selective visual attention. *Annu Rev Neurosci*, 18:193–222, 1995.

[6] J.H. Reynolds, T. Pasternak, and R. Desimone. Attention increases sensitivity of v4 neurons. *Neuron*, 26(3):703–14, 2000.

[7] F. H. Hamker and M. Zirnsak. V4 receptive field dynamics as predicted by a systems-level model of visual attention using feedback from the frontal eye field. *Neural Netw*, 19(9):1371–1382, 2006.

[8] F. H. Hamker. The reentry hypothesis: linking eye movements to visual perception. *J Vis*, 3(11):808–816, 2003.

[9] J.H. Reynolds and D.J. Heeger. The normalization model of attention. *Neuron*, 61(2):168–85, 2009.

[10] R. Gattass and C.G. Gross. Visual topography of striate projection zone (mt) in posterior superior temporal sulcus of the macaque. *J Neurophysiol*, 46(3):621–38, 1981.

[11] T D Albright and R Desimone. Local precision of visuotopic organization in the middle temporal area (mt) of the macaque. *Exp Brain Res*, 65(3):582–92, 1987.

[12] J.R Cavanaugh, W. Bair, and J.A. Movshon. Nature and interaction of signals from the receptive field center and surround in macaque v1 neurons. *J Neurophysiol*, 88(5):2530–46, 2002.

[13] M.P. Sceniak, M.J. Hawken, and R. Shapley. Visual spatial characterization of macaque v1 neurons. *J Neurophysiol*, 85(5):1873–87, 2001.